

Low lying spectroscopy of odd-odd ^{146}Eu

T. Bhattacharjee,^{1,*} D. Banerjee,² S. K. Das,² T. Malik,³ S. Chanda,⁴
A. Chowdhury,¹ P. Das,¹ S. Bhattacharyya,¹ and R. Guin²

¹Variable Energy Cyclotron Centre, Kolkata - 700064, India

²RCD-BARC, Variable Energy Cyclotron Centre, Kolkata - 700 064

³Department of Applied Physics, Indian School of Mines, Dhanbad, India

⁴Fakir Chand College, Diamond Harbour, West Bengal, India

(Dated: April 24, 2019)

The γ spectroscopy for the low lying states of $N=83$ Eu isotope has been performed from EC decay of $^{146}\text{Gd}(\tau_{1/2} = 48 \text{ days})$, produced by $^{144}\text{Sm}(\alpha, 2n)$ reaction with 32 MeV alpha beam from $K = 130$ cyclotron at Variable Energy Cyclotron Centre, Kolkata. The level structure has been significantly modified from the measurement of γ singles, $\gamma - \gamma$ coincidence and decay half lives. Lifetime measurement has been performed for the 3^- , 114.06 keV and 2^- , 229.4 keV levels of ^{146}Eu , by using Mirror Symmetric Centroid Difference (MSCD) method with LaBr_3 detectors. Mean lifetimes of $5.38 \pm 1.8 \text{ ps}$ and $8.38 \pm 1.6 \text{ ps}$ have been determined respectively for these two states. A shell model calculation has also been performed using OXBASH code.

PACS numbers: 21.10.-k; 21.10.Tg; 21.60.Cs; 23.20.Lv; 29.30.Kv; 29.40.Wk; 29.40.Mc;

Keywords: Fusion evaporation reaction $^{144}\text{Sm}(^4\text{He}, 2n)$, $E_{\text{beam}}=32 \text{ MeV}$; measured E_γ , I_γ , $\gamma\gamma$; Lifetime, MSCD method; ^{146}Eu low spin states; $\text{LaBr}_3(\text{Ce})$, HPGe detector; shell model, OXBASH calculation;

I. INTRODUCTION

The focus on the nuclear structure physics has taken a different direction until very recently, after a prolonged exploration on high spin phenomena. Instead of populating and exploring high spin structure of the nuclei, a renewed interest is being observed towards the low-lying spectroscopy. This has indeed been possible because of the availability of the suitable detection systems with high energy and time resolution due to the progress in modern day research on detector technology. Many nuclei are being revisited with different types of experimental setups in order to probe the phenomena enriching the low lying structure of nuclei, viz., tetrahedral deformation [1] or shape coexistence [2, 3]. At the same time, the importance is also being realized for furnishing a complete information on all the observables other than the level energy and spin parity, viz., lifetime and transition moments, in deciding the structure of a particular nucleus.

Over the years, significant interest has been attracted by the low lying structure of odd-odd transitional nuclei in $A \sim 140$ region. This is because of the similarity of available orbitals for protons and neutrons as both occupy the 50-82 sub-shell space. The interaction amongst these orbitals and the interplay of collective and single particle excitation in this mass region has been a topic of experimental as well as theoretical exploration since many years [4–7]. These nuclei have provided a perfect ground for studying the excited states having contribution of both the single particle

and collective modes of excitation, thus carrying a measurable degree of two kinds of transition moments. Though low lying excited states have been studied from off-beam decay and in-beam experiments with light ion beams, the information on level lifetimes and specifically the transition moments have been very rare in almost all the nuclei. The studies have been performed mostly with the $\text{NaI}(\text{Tl})$ scintillation detectors or with intrinsic $\text{Ge}(\text{Li})$ detectors having limited efficiency and resolution of gamma ray detection. Thus there is a remaining scope to revisit many of these nuclei [3] in order to complete these informations of the low lying states including their lifetime and transition moments. This may reveal important information regarding the different modes of excitation and their involvement in the underlying structure of these nuclei.

The nuclear level lifetime is one of the most critical parameters in nuclear spectroscopy as this provides a direct insight into the structure of a level. The measurements of lifetimes, which are estimated to be of the order of several ones or tens of picoseconds, require a detecting system having a very good time resolution as well as a moderate energy resolution. The precise technique for the measurements of level lifetimes of the order of few picoseconds and having a complex decay scheme has been a topic of research for many years [8, 9]. Due to the availability of $\text{LaBr}_3(\text{Ce})$ detectors in very recent times, such measurements have taken a new direction [10]. Above all, the availability of light ion beams from the $K = 130$ cyclotron at Variable Energy Cyclotron Centre, Kolkata has opened the possibility of experimental research in this particular direction.

* Corresponding author; btumpa@veccal.ernet.in

The odd-odd nuclei, close to $Z=64$ and $N=82$ shell

closure, have single particle structure involving the particle(hole)-hole(particle) excitation of proton and neutron. The odd-odd ^{146}Eu , with one extra particle compared to the neutron shell closure at $N=82$, is interesting in order to test the validity of the very well known subshell closure at $Z=64$, as observed in ^{146}Gd [11]. The structure of the ^{146}Eu has been studied both from off-beam decay measurement and in beam γ spectroscopy with light particle and HI beams as well as single particle transfer reactions [12–18]. The off beam decay measurements have been explored by different groups in order to develop the excited levels as well as to measure their lifetimes. Out of these, R. Kantus et al. have done coincidence measurements with a Ge(Li) and a Gam-X detector and developed a level scheme up to 690.7 keV excitation [14]. However, there is a wide variation in the information on the populated levels, γ rays decaying from these levels and their intensities obtained from the different measurements on ^{146}Gd EC decay. The suggested sequence of the low lying states has been accounted for by combining a $d_{5/2}$ proton hole and a $f_{7/2}$ neutron particle following the jj coupling scheme of odd-odd nuclei. The spins of the excited states are reproduced by the recoupling of the ground state configuration $[(\pi d_{5/2})(\nu f_{7/2})]_{4-}$ and is conjectured from the observation of the high spin members of the $\pi d_{5/2}^{-1}\nu f_{7/2}$ and $\pi g_{7/2}^{-1}\nu f_{7/2}$ multiplets in the in beam study of ^{146}Eu . The 9^+ , 235 μs isomeric state has been identified from the in beam study with ^{12}C beam and its decay has been rigorously studied by Ercan et al., identifying the population of higher multiplets of the $(\pi d_{5/2})(\nu f_{7/2})$ configuration [15]. Two particle-phonon multiplet states of configuration $\pi h_{7/2} \nu f_{7/2} \times 3^-$ and four nucleon yrast states have been identified at around 2 MeV and above by Ercan et al [16]. E. Ideguchi et al have studied the high spin states up to 10 MeV and identified a ns isomer around 8 MeV [17], by populating the nucleus with ^{10}B beam. Even there exists a range of studies for the excited states of ^{146}Eu , the decay studies of ^{146}Gd have been done with limited experimental setups with Ge(Li) detectors. The lifetime of the first 3^- and 2^- states has been measured by L. Holmberg et al. by using electron-electron coincidence measurement in a magnetic spectrometer and with plastic detectors [13]. However, the sequence of the two important 114 and 115 keV γ transitions has been modified afterwards. Moreover, the lifetime of the 3^- state varies from 0.2 ns to 0.8 ns as obtained from different measurements [12]. In addition, the lifetimes of the above two excited states seems to be quite large considering the suggested configuration of these states. The study of the lifetime can reveal important information on the underlying configurations. Also a shell model calculation will be quite appropriate in order to characterise the experimental observations on these states and there is no light till date on this issue.

In the present work, we have reported the low lying

structure of odd-odd ^{146}Eu nucleus by populating its excited states from the EC decay of ^{146}Gd with a half life of 48 days. The decay spectroscopy has been performed with the measurements of γ singles, $\gamma-\gamma$ coincidence and the decay half lives. New gamma rays have been observed both in the singles and the coincidence data modifying the decay scheme of ^{146}Gd significantly. The lifetime of the first 3^- and 2^- states have been measured with LaBr_3 (Ce) detectors by using mirror symmetric centroid difference (MSCD) method [10]. A shell model calculation has also been performed using OXBASH code [20] in order to characterise the low lying structure of ^{146}Eu .

II. EXPERIMENTAL DETAILS

The excited states of ^{146}Eu have been populated from the EC decay of ^{146}Gd ($t_{1/2} = 48$ days), produced via $^{144}\text{Sm}(\alpha, 2n)^{146}\text{Gd}$ reaction with 32 MeV alpha beam from K=130 Cyclotron at Variable Energy Cyclotron Centre, Kolkata. The ^{144}Sm targets with a thickness of 300 $\mu\text{g}/\text{cm}^2$ were prepared on 6.84 mg/cm^2 Al foils by electro-deposition of 97% enriched Sm_2O_3 . The ^{146}Gd nuclei produced from the above reaction were recoil-implanted on Al catcher foils (6.84 mg/cm^2) for the subsequent measurements. The Al catcher foils containing the Gd activity were dissolved in NaOH and the ^{146}Gd was co-precipitated with Fe-hydroxide from the alkaline solution. The precipitate, after washing with water, was dissolved in 9(M) HCl and the ^{146}Gd activity was separated in carrier-free form by column-chromatographic separation technique. The separated ^{146}Gd activity in acid solution was subsequently used for $\gamma-\gamma$ coincidence and lifetime measurements. The irradiated target was used for the measurements of γ singles and decay half lives with a 50% HPGe detector. In this measurement, the target was kept at a distance of 15 cm from the detector to ensure a dead time less than 10% and hence to minimise the summing effect. A digital system was used for biasing, pulse processing and data collection of the 50% HPGe detector. The $\gamma-\gamma$ coincidence data were acquired with a setup (called as ‘Ge-setup’ in this paper) consisting of one 10% single HPGe detector and a segmented Low Energy Photon Spectrometer (LEPS), kept at an angle of 180° with respect to each other. Another setup (called as ‘LaBr₃-setup’ in this paper) consisting of three 30 mm x 30 mm LaBr_3 (Ce) detectors was used for the measurement of lifetimes. In this setup, one detector was used as ‘START’ detector and the other two detectors, kept at 90° and 180° with respect to the ‘START’ detector, were used as the ‘STOP’ detectors. Hence, two Time to Amplitude (TAC) signals were generated corresponding to the two ‘STOP’ detectors. However, only one TAC signal from the 180° ‘STOP’ detector was used for the present measurement. In both the coincidence setups, used for $\gamma-\gamma$ coincidence (Ge-setup) and lifetime measurements (LaBr₃-setup), 8K ADC and CAMAC based data acquisition system were used for collecting the zero

suppressed list mode data with LAMPS [21] software. The absolute efficiency of all the HPGe and LEPS detectors, required for the measurement of γ -ray intensity, were determined by using ^{152}Eu and ^{133}Ba sources with known activity.

III. DATA ANALYSIS AND RESULTS

The data analysis has been performed for the (i) measurements of decay half lives with the 50% HPGe detector, (ii) $\gamma - \gamma$ coincidence measurements using Ge-setup and (iii) lifetime measurements using LaBr₃-setup. The detailed procedures have been discussed in the following subsections along with the obtained results.

A. Decay measurements and $\gamma - \gamma$ coincidence measurements

The singles γ spectra acquired with the 50% HPGe detector, for a duration of 48h in each run and at definite time intervals, have been studied for the assignment of gamma rays in the level scheme of ^{146}Eu . All the γ rays observed in the total spectra, as shown in FIG. 1, were identified and the gamma rays, relevant to the level scheme of ^{146}Eu , were studied for the decay half lives. This data was also used for the measurement of energy and intensity of the transitions. The gamma rays observed in the total spectrum can be classified in three categories, viz., (i) the gamma rays of ^{146}Eu , (ii) gamma rays of ^{146}Sm , produced from the EC decay of ^{146}Eu , and (iii) the background gamma rays along with possible X-rays. The γ rays of later two categories were not considered in the present work. In addition, the γ rays of ^{146}Eu , having energies below the EC decay Q value of ^{146}Gd , were only used for the development of the decay scheme of ^{146}Gd . The decay plots for the relevant gamma rays have been shown in FIG. 2. The coincidence information has been derived from the data taken with the Ge-setup with the carrier-free ^{146}Gd activity. The gates were placed on 114.06, 114.88, 153.86, 267.02 and 268.96 keV transitions in the spectrum (shown in FIG. 3) of LEPS detector and the projected spectra obtained in the 10% HPGe detector have been shown in FIG. 4 and 5. In the present work, only 114.06, 114.88, 153.86, 267.02 and 268.96 keV transitions, out of all the γ rays reported for the decay of ^{146}Gd [12], were observed both in the coincidence as well as singles data. It is observed that 114.06 keV and 114.88 keV transitions are in coincidence with one another and also in coincidence with the 153.86 keV transition. The 229.4 keV transition is observed only in the gate of 153.86 keV but not in the gates of 114.06 and 114.88 keV transitions. The 268.96-keV transition has been observed only in the gate of 114.06 keV but not in 114.88 and 153.86 keV gates. The overlapped spectra of 267.06 and 268.96 keV transitions show that only 114.06 keV is present in the 268.96 keV gate whereas both the 114.06 and 114.88

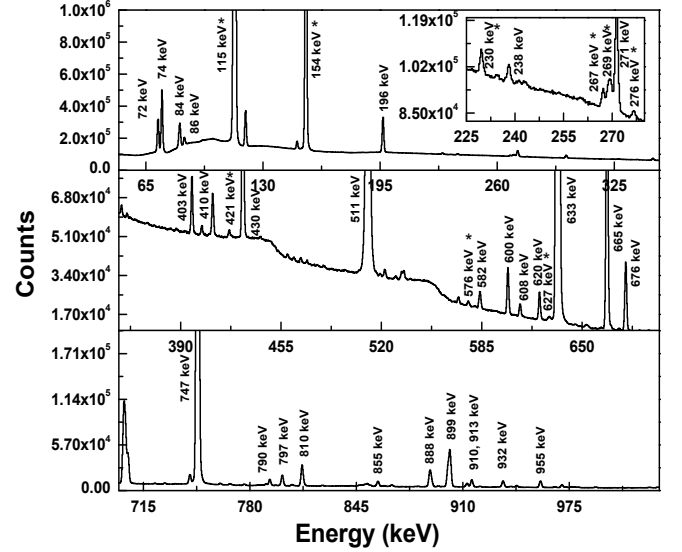


FIG. 1. The decay γ spectrum obtained with the 50% HPGe detector. γ rays upto the EC decay Q value have been shown in the figure. The peaks marked with * belong to ^{146}Eu .

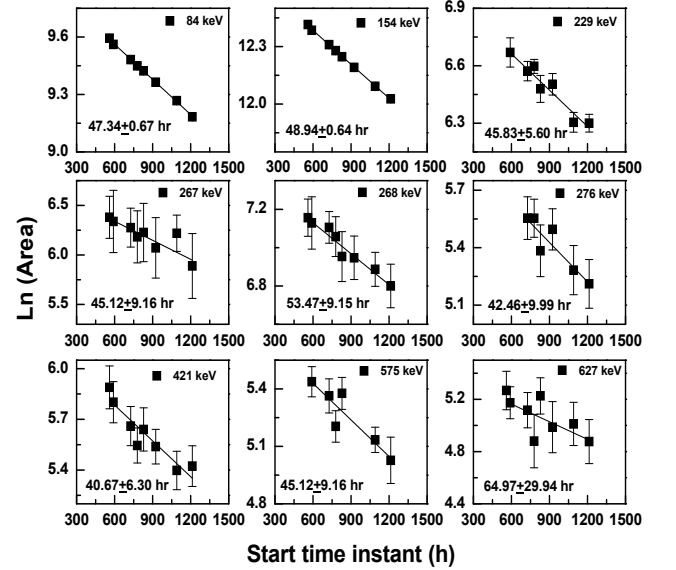


FIG. 2. The decay plots of the γ transitions corresponding to EC decay of ^{146}Gd . The γ energy and the half life value have been indicated inside each figure.

keV transitions are present in the 267.06 keV gate. The aforesaid observation is also supported with the fact that the FWHM value for the peak obtained in the 267.06 keV gate is higher than that obtained in 268.96 keV gate. From these observations, the placements of the 114.06, 114.88, 153.86 and 267.06 keV gamma rays were confirmed. The measured half lives of 229.4 and 268.86 keV transitions in the present work rule out the possibility of these two transitions to be originated from the summing

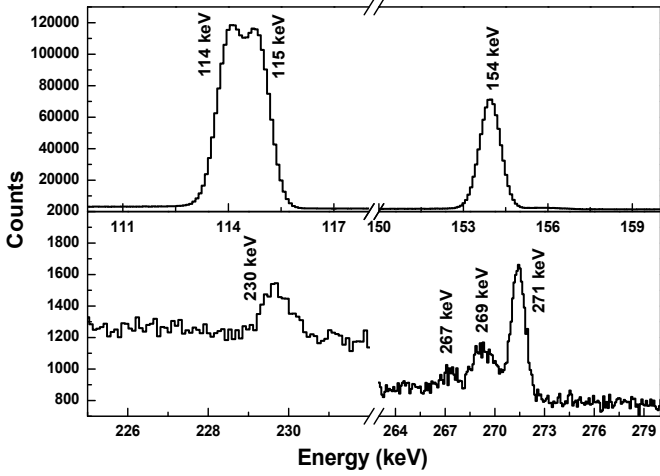


FIG. 3. The spectrum obtained with one segment of the LEPS detector in Ge-setup.

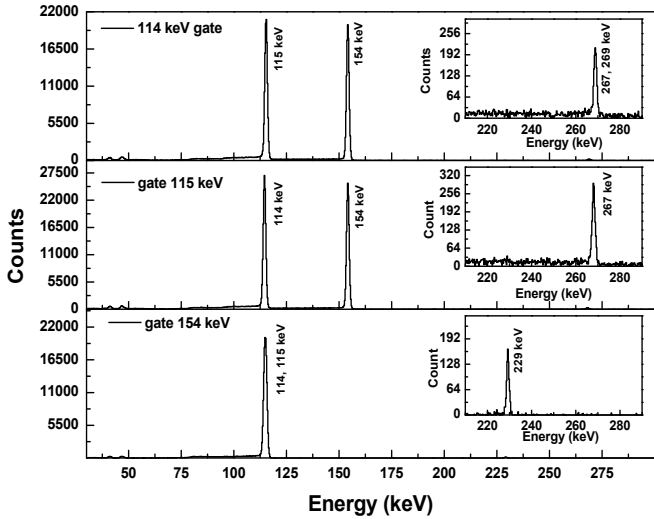


FIG. 4. The gated spectra obtained from the 10% HPGe detector by putting gate on 114.06 keV (top), 114.88 keV (middle) and 153.86 keV (bottom) in the LEPS detector. The insets show the region from 210 keV to 290 keV in an expanded scale.

effect. The 229.4 keV and 268.86 keV transitions were included parallel to the 114.06-114.88 keV and 114.88-153.86 keV cascades respectively, as evident from their coincidence data and decay half lives explained above. The 420.88 and 575.24 keV γ rays were observed in the singles data and their half lives confirm their placement in the level scheme. There was no indication of the 76 keV and 383 keV γ rays, either in the coincidence data or in the singles data, and hence these two transitions were rejected from the level scheme. The 84.01, 276.57 and 627.35 keV gamma rays have been observed in the

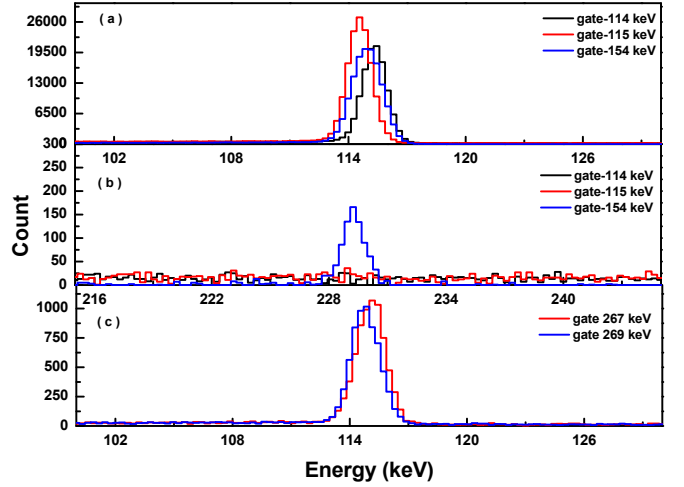


FIG. 5. The gated spectra obtained from the 10% HPGe detector by putting gates on 114.06 keV, 114.88 keV, 153.86 keV, 267.02 keV and 268.96 keV in LEPS detector are overlapped. Different energy regions of interest are shown in expanded scale.

singles data of the present work and show the half lives of ~ 48 days. The first two transitions, viz. 84.01 and 276.57 keV, are reported to be produced from the decay of the $235 \mu\text{s}$ isomer as well as from the heavy ion fusion evaporation work [17]. Again these two γ rays are reported to be present in the 14-276-84-276 keV cascade according to the adopted level scheme of the nucleus. Between the two placements of the 276 keV transition, as decided by the above cascade, the one feeding the 84 keV γ ray is reported to be decaying from the 647.5 keV level. However, the strongest transition decaying from this 647.5 keV level is 358 keV which was not found to exist in our data. Hence, the second 276 keV transition is not originated from the EC decay of ^{146}Gd and is excluded from the decay scheme of the present work. Again, the calculated intensity of the 627.35 keV transition comes out to be equal to that of 276.57 keV transition. This observation suggests that the 627.35 keV transition is the one which is reported as 624.5 keV [12] decaying from the 914 keV level (modified as 918.5 keV level in the present work). Hence, it is concluded that the 918.5 keV level is produced from the EC decay of ^{146}Gd and then feeds the 14.57-276.57-627.35 keV cascade. A very high value of intensity ($\sim 12\%$) for the 84.01 keV transition does not support it to be feeding the 276 keV γ ray which subsequently feeds the 14 keV level. This observation, along with the similar intensity of 627.35 and 276.57 keV transitions as explained above, excluded the 84.01 keV transition from the present decay scheme. Based on all these information, the decay scheme of ^{146}Gd has been modified significantly and shown in Fig. 6. The energy and absolute intensity of the γ rays belonging to ^{146}Eu have been calculated from the singles measurement with

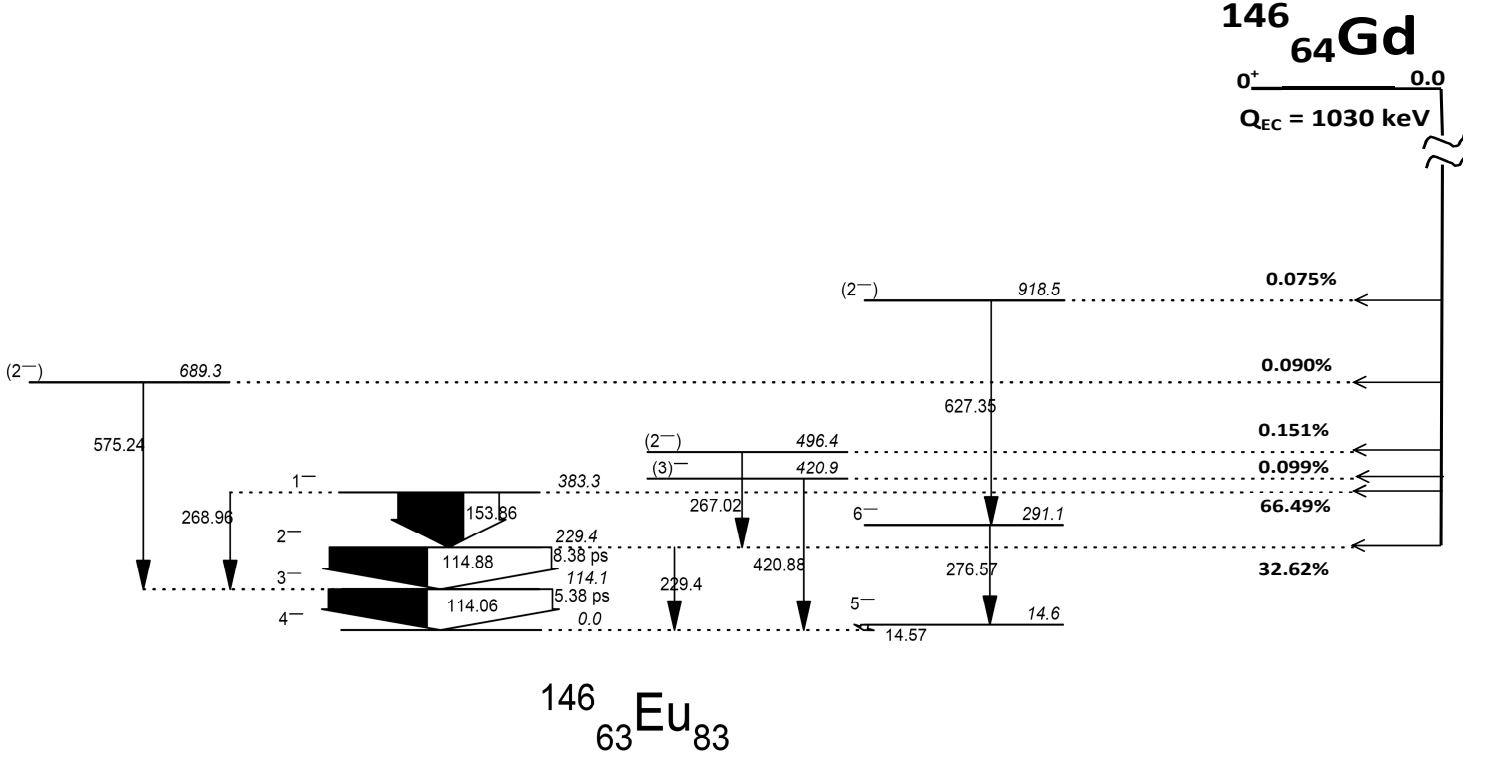


FIG. 6. The level scheme of ^{146}Eu from the decay of ^{146}Gd , as obtained from the present work.

50% HPGe detector and indicated in TABLE I. While calculating the intensities, it has been considered that the intensities of the 14, 114.06, 229.4 and 420.88 keV transitions, feeding the ground state of ^{146}Eu , add up to 100%. Due to the fact that the 114.06 and 114.88 keV peaks could not be separated, the combined intensity of these two transitions was calculated from the total area obtained in the singles data. This total intensity has been distributed among these two energies according to the following equations by considering that no direct EC decay is feeding the 114.06 keV level.

$$I_{114} + I_{115} = I_{total} \quad (1)$$

and

$$I_{114} = I_{115} + I_{575} + I_{269} \quad (2)$$

The ratio of intensity for 114.06 keV to that for 114.88 keV transition has also been verified from the total spectrum obtained in one segment of the LEPS detector as the two peaks could be nicely separated with this detector. The intensity of the 14 keV transition has been considered to be equal to that of 627.35 keV as discussed above. However, the intensity of 14 keV transition is

much smaller than that of 114.06 keV and lies within the error limit. The normalised intensities have been used in order to develop the decay scheme of ^{146}Gd ground state to different levels of ^{146}Eu as shown in Fig. 6. The $\log F\tau$ values have been calculated from the LogFt calculator of NNDC [19] for different EC decays and have been shown in TABLE I. These values have been used in the assignment of J^π for the states populated in ^{146}Gd decay. The spin parity of all the states was kept unchanged with respect to the adopted decay scheme [12] except the 917.9 keV level which has been assigned to a J^π value of 2^- . The obtained half lives, important in order to identify the γ rays involved in the decay of ^{146}Gd , have also been shown in the same TABLE I.

B. Lifetime Measurements

The lifetimes of the excited levels of ^{146}Eu was measured following the mirror symmetric centroid difference (MSCD) method proposed by Regis et al [10]. The conventional centroid shift method [8, 9] is limited by the fact that the prompt reference curve depends on the gamma ray energy. In case, the prompt references are not known

TABLE I. The populated levels of ^{146}Eu from the EC decay of ^{146}Gd .

E_i	$J_i^\pi \rightarrow J_f^\pi$	E_γ^a	I_γ^b	half life	Ec feeding (%)	$\text{LogF}\tau^c$
14.6	$5^- \rightarrow 4^-$	14.0	$0.075(\pm 0.011)$	-	-	-
114.1	$3^- \rightarrow 4^-$	114.06	$99.64 (\pm 3.21)$	48.3 ± 0.31^d	-	-
229.4	$2^- \rightarrow 3^-$	114.88	$98.74 (\pm 3.18)$	48.3 ± 0.31	32.63	7.8
383.3	$1^- \rightarrow 2^-$	153.86	$66.16 (\pm 1.02)$	48.94 ± 0.64	66.52	7.3
229.4	$2^- \rightarrow 4^-$	229.4	$0.188 (\pm 0.009)$	45.83 ± 5.6	32.63	7.8
496.4	$(5^-) \rightarrow 4^-$	267.02	$0.151 (\pm 0.029)$	45.11 ± 9.16	0.151	9.7
383.3	$1^- \rightarrow 3^-$	268.96	$0.335 (\pm 0.027)$	53.47 ± 5.15	66.52	7.3
291.1	$6^- \rightarrow 5^-$	276.57	$0.067 (\pm 0.007)$	42.46 ± 9.99	-	-
420.9	$(3^-) \rightarrow 4^-$	420.88	$0.099 (\pm 0.011)$	40.63 ± 6.3	0.099	10
689.3	$(2^-) \rightarrow 3^-$	575.24	$0.090 (\pm 0.008)$	45.12 ± 9.16	0.090	9.5
918.5	$(2^-) \rightarrow 6^-$	627.35	$0.075 (\pm 0.011)$	64.16 ± 29.9	0.075	8.4

^a The γ energies have been obtained with an error of ≤ 0.5 keV.

^b The errors in the efficiencies and the area under the photopeaks have been considered for calculating the error in the intensities. The conversions coefficients have been considered for low energy transitions. The values of the coefficients have been obtained for the Brice calculator of NNDC.

^c The $\text{LogF}\tau$ values have been calculated from the $\text{LogF}\tau$ calculator of NNDC.

^d As the 114 and 115 keV peaks could not be separated in the spectrum obtained with the 50% HPGe detector, both the peaks were considered while calculating the half life.

or can not be extended for the gamma rays of interest with the standard sources, the Compton-Compton events are used for generating the prompt curves. Because of the inherent delay between a Compton-Compton and a photopeak-photopeak coincidence event, added up with other spurious events, such prompt curves are shifted significantly from the true prompt line and affect the measurements of lifetimes \sim few ps [9]. Whereas, in MSCD method, the lifetime can be derived as a function of the energy difference between the two gamma rays which are feeding to and decaying from the level of interest. Due to this fact, the MSCD technique allows the use of both the photopeak-photopeak and Compton-Compton events for the generation of prompt curves. Following the conventional centroid shift method the lifetime τ of a specific branch is given by,

$$\tau = C(D)_{\text{stop}} - C(P)_{\text{stop}} = -C(D)_{\text{start}} + C(P)_{\text{start}} \quad (3)$$

where $C(D)_{\text{start}}$ and $C(D)_{\text{stop}}$ are the TAC centroids of the delayed coincidence when references are taken from start detector and stop detector respectively. $C(P)_{\text{start}}$ and $C(P)_{\text{stop}}$ are similar TAC centroids for the prompt coincidences obtained from a prompt reference source. The $C(P)_{\text{start}}$ (or $C(P)_{\text{stop}}$), obtained by varying the γ energy gates in the stop(or start)detector, generates the prompt reference curve when plotted as a function of the those γ energy values. The corresponding centroid of the level of interest ($C(D)_{\text{start}}$ or $C(D)_{\text{stop}}$) is shifted from the prompt reference curve by the level lifetime (τ). Whereas, the MSCD technique modifies this centroid shift method in the following way:

$$\begin{aligned}
\Delta C(D) &= C(D)_{\text{stop}} - C(D)_{\text{start}} \\
&= \tau + C(P)_{\text{stop}} + \tau - C(P)_{\text{start}} \\
&= 2\tau + C(P)_{\text{stop}} - C(P)_{\text{start}} \\
&= 2\tau + \Delta C(P)
\end{aligned} \quad (4)$$

In this technique, the Prompt Reference Distribution (PRD) is generated from the plot of $\Delta C(P)$ against the ΔE_γ (difference in the γ energies between one feeding to and that decaying from a prompt level) using a prompt source, as explained in ref. [10]. For a particular value of ΔE_γ , the $\Delta C(D)$, obtained from a delayed source, is shifted by twice the lifetime of the level of interest (2τ) from the PRD curve as explained in the equation 4.

In this work the ‘START’ and ‘180°-STOP’ detectors in the LaBr₃-setup were used for the measurement of lifetimes of first 3^- and 2^- levels of ^{146}Eu . Temperature stability was maintained in the experimental area to ensure a steady timing electronics. The ^{60}Co prompt source was used to generate the PRD curve and the accuracy of our experimental setup was established with the measurement of 32.4 ps lifetime for the 344.2 keV level of ^{152}Gd produced from the β^- decay of ^{152}Eu source. The 344.2 keV level decays by a 344.2 keV gamma ray to the ground state of ^{152}Gd and is fed by several gamma rays as known from its adopted level scheme [22]. The PRD curve was generated by using the Compton profile of the ^{60}Co source with the reference energy gate at 344 keV in the ‘START’ (‘STOP’) detector. In the ‘STOP’ (‘START’) detector, a ~ 10 keV wide energy gate was selected in the Compton profile of ^{60}Co source in 10 keV intervals. The different coincident photopeaks of ^{152}Gd have been projected (shown in FIG. 7) in the spectrum of ‘START’ detector by putting gate at 344 keV in the 180° ‘STOP’ detector. Due to the desired energy resolution of the LaBr₃(Ce) detector, all the peaks could be clearly identified. The TAC spectra were obtained with the gate at 344 keV photopeak in the 180° ‘STOP’ detector and the gates at the other photopeaks, in coincidence with 344 keV, given in the ‘START’ detector. Some of these TAC spectra have been shown in Fig. 8 in order to envisage the dependence of the TAC centroid on the

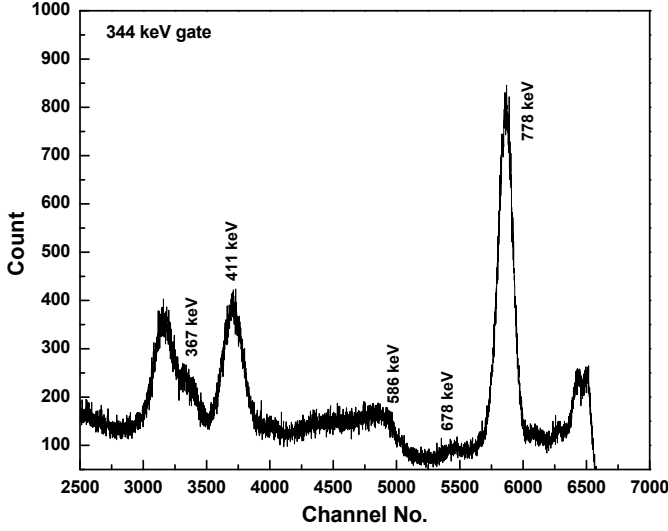


FIG. 7. The γ spectrum obtained with the ‘START’ LaBr₃ detector, when a 344 keV gate is placed in the 180° ‘STOP’ detector.

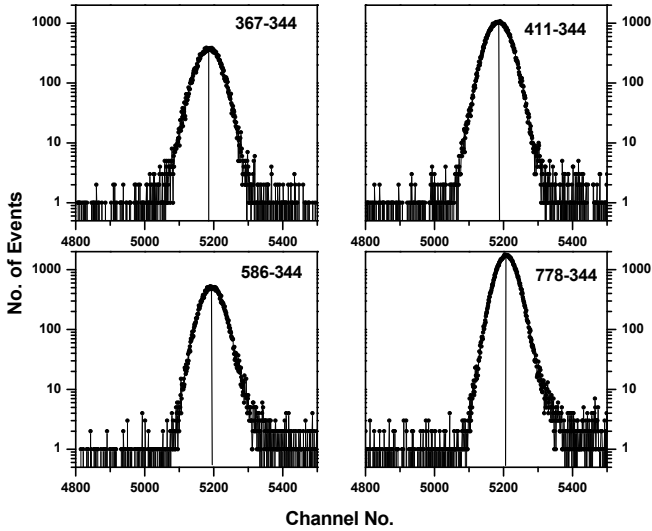


FIG. 8. The TAC spectra obtained with 344 keV ‘STOP’ gate in the 180° detector and different ‘START’ gates with γ transitions feeding the 344 keV level of ^{152}Eu . The increase in the TAC centroid are clearly visible.

γ energy. Similar TAC spectra were obtained with the 344 keV gate at the ‘START’ detector and other photopeaks at the ‘STOP’ detector. The Fig. 9 represents the difference in the TAC centroids obtained by interchanging the ‘START’ and ‘STOP’ energy gates with a special reference to the 411-344 and 778-344 keV cascades. The similar differences in the TAC centroid were also obtained for the other cascades of ^{152}Gd and have been utilized for the measurements of the lifetime of 344.2 keV level. The PRD curve, generated with the ^{60}Co source, has been shown in Fig. 10 and fitted with a func-

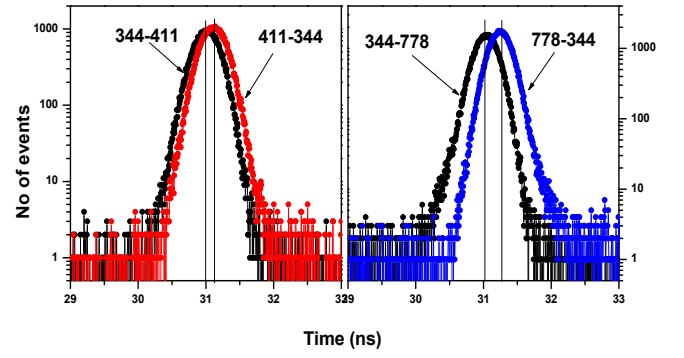


FIG. 9. The TAC spectra obtained with ‘START’ and ‘STOP’ gates for the 344 keV level of ^{152}Eu have been overlapped for two γ transitions, viz., 411 keV and 778 keV.

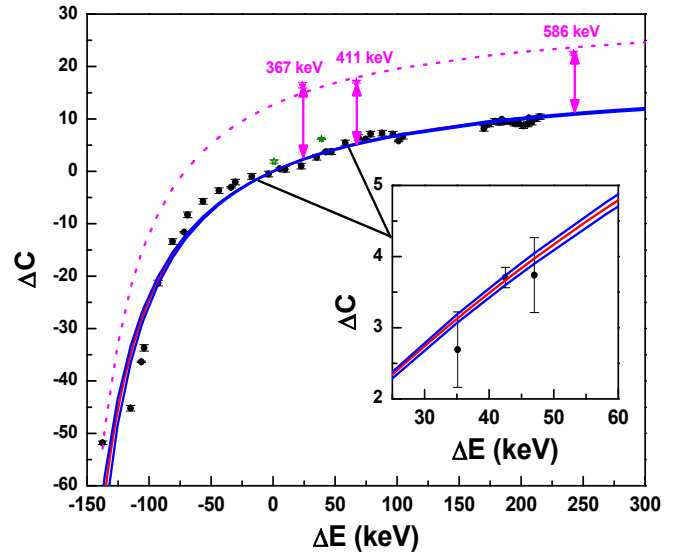


FIG. 10. The PRD curve generated by fitting the data points of ^{60}Co (black circles) has been shown with a solid red line. The two solid blue lines show the upper and lower limits of the prompt curve. The data points for 344 keV level of ^{152}Gd have been shown by pink \star s. The pink line approximately shows a shift of 34 ps from PRD curve. A selected portion of PRD curve has been zoomed and shown in inset.

tion $f(\Delta E_\gamma) = \frac{a\Delta E_\gamma}{b + \Delta E_\gamma}$, where a and b comes out to be 18.96 ± 0.145 and 177.3 ± 2.39 respectively. The fitted curve has been shown with red solid line. The two blue dotted lines show the positive and negative limits of this prompt curve by calculating them from the errors obtained in the fitting parameters. It is observed that the prompt curve can be determined within a limit of 3 ps on an average, except for a very large negative values of ΔE_γ . The ΔC values obtained for 367-344, 411-344 and 586-344 cascades of ^{152}Gd have also been shown in the

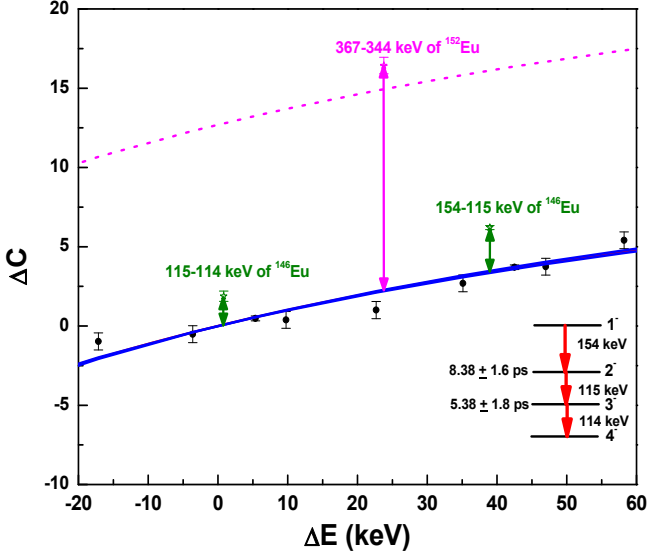


FIG. 11. Fig. 10 has been shown in expanded scale for a close view of the centroid differences obtained for the energy levels of ^{146}Eu . The green *s have been added which are the data points obtained for 114.06 keV and 229.4 keV levels of ^{146}Eu .

same figure. The shift of these data points from the PRD curve gives $\tau = 37.68 \pm 3.3$ ps, which is in well agreement with the literature value (32 ps) for the lifetime of 344 keV level of ^{152}Gd . However, the similar shifts for the 658-344 and 778-344 cascades show a higher value (~ 60 ps) for the lifetime of this 344 keV level. This is probably because of the non linearity observed in the energy response of the LaBr_3 (Ce) detector at higher energy values under the present working voltages of the photo-multiplier tube. After the lifetime for the 344 keV level of ^{152}Gd was reproduced very accurately, the similar centroid differences were also obtained for the level of ^{146}Eu and also shown in Fig. 10. The 114.06-114.88 and 114.88-153.86 keV cascades were used for deducing the lifetimes of first 3^- and 2^- states of ^{146}Eu . In Fig. 11, the ΔC values obtained for the ^{146}Eu have been shown with respect to the PRD curve of Fig. 10, in an expanded scale. In TABLE II the centroid differences for the different cascades of ^{146}Eu and ^{152}Eu have been tabulated and the obtained lifetimes have been shown for the corresponding levels.

IV. SHELL MODEL CALCULATION

A large basis shell model calculation was performed using the code OXBASH [20] in order to characterize the low-lying states of ^{146}Eu . The calculation considered ^{132}Sn as core and thirteen protons distributed over the model space comprising of $\pi(1g_{7/2}, 2d_{5/2}, 2d_{3/2},$

TABLE II. The lifetime of the first two excited levels of ^{146}Eu and the 344 keV level of ^{152}Eu , obtained from the present work.

Nucleus	Cascade	ΔC	PRD	τ (ps)
^{152}Eu	(367-344)keV	16.43	2.24	42.56 ± 2.2
	(411-344)keV	17.11	5.21	35.7 ± 1.7
	(586-344)keV	22.54	10.94	34.78 ± 1.8
^{146}Eu	(115-114)keV	1.88	0.087	5.38 ± 1.8
	(154-115)keV	6.21	3.42	8.38 ± 1.6

$3s_{1/2}$) single particle orbitals along with one neutron over the $\nu 1f_{7/2}$ single particle orbital. The calculations were carried out using proton-neutron formalism in full particle space. The two-body matrix elements were obtained from the well-known *N82POTA* interaction supplied with the source code of OXBASH. This interaction is basically a combination of *ROTANN*, *ROTAPP* and *ROTAPN* interaction files which are also supplied with the code. The *ROTAPP* TBMEs were obtained by Brown et al. [23] by a 5-parameter fit to *H7B* interaction [24] potential for $N=82$ core and the corresponding NN TBMEs were obtained in the same way but by excluding the Coulomb interaction. The bare G matrix from the *H7B* was used for the PN TBMEs. In our calculations, we have truncated the neutron space to contain only $1f_{7/2}$ orbital as well as the proton space by excluding the $1h_{11/2}$. In the *N82POTA* interaction, the neutron single particle energies (SPEs) were chosen to give the -7.48 MeV energy difference between ^{147}Gd and ^{146}Gd as well as to best reproduce the excitation energies of $\frac{7}{2}$, $\frac{9}{2}$ and $\frac{13}{2}$ states in ^{149}Dy spectrum. The proton SPEs were obtained from the potential fit as mentioned above. The lifetime values have been determined from the reduced transition probabilities obtained from the calculation, for different excited states of ^{146}Eu .

TABLE III shows calculated excitation energies of the negative parity states up to the 1^- level at 383.3 keV along with the theoretical and experimental lifetimes and the major configuration of the states. A remarkable agreement for the energies and lifetimes is noticeable. It is also noticeable that the major contribution to the structure of the states comes from the $\pi g_{7/2}$ and $\pi d_{5/2}$ orbitals which constitute the ^{146}Gd core ground state.

V. DISCUSSION

The decay spectroscopy of ^{146}Gd nucleus has been performed using the light ion beams from Variable Energy Cyclotron Centre to study the low lying structure of the odd odd ^{146}Eu nucleus. The low lying excited

TABLE III. The level energies and lifetimes have been compared with shell model calculation. The major configurations responsible for the low lying levels of ^{146}Eu have been shown as obtained from the said calculation.

J^π	E_{level} (keV)		Lifetime (ps)		Configuration
	(expt)	(theory)	(expt)	(theory)	
4^-	0.0	0.0	-	-	$[\pi(g_{\frac{7}{2}}^8, d_{\frac{5}{2}}^5)\nu(f_{\frac{7}{2}})^1]$ 82% + $[\pi(g_{\frac{7}{2}}^8, d_{\frac{5}{2}}^4, d_{\frac{3}{2}}^1)\nu(f_{\frac{7}{2}})^1]$ 12.3% + $[\pi(g_{\frac{7}{2}}^8, d_{\frac{5}{2}}^4, s_{\frac{1}{2}}^1)\nu(f_{\frac{7}{2}})^1]$ 4.1%
5^-	14.0	4.0	-	-	$[\pi(g_{\frac{7}{2}}^7, d_{\frac{5}{2}}^6)\nu(f_{\frac{7}{2}})^1]$ 77.3% + $[\pi(g_{\frac{7}{2}}^7, d_{\frac{5}{2}}^4, d_{\frac{3}{2}}^2)\nu(f_{\frac{7}{2}})^1]$ 15.2%
3^-	114.06	119	5.38 ± 1.8	5.5	$[\pi(g_{\frac{7}{2}}^7, d_{\frac{5}{2}}^6)\nu(f_{\frac{7}{2}})^1]$ 62.7% + $[\pi(g_{\frac{7}{2}}^8, d_{\frac{5}{2}}^5)\nu(f_{\frac{7}{2}})^1]$ 20% + $[\pi(g_{\frac{7}{2}}^7, d_{\frac{5}{2}}^4, d_{\frac{3}{2}}^2)\nu(f_{\frac{7}{2}})^1]$ 11.5%
2^-	229.4	232	8.38 ± 1.6	4.6	$[\pi(g_{\frac{7}{2}}^8, d_{\frac{5}{2}}^5)\nu(f_{\frac{7}{2}})^1]$ 63.8% + $[\pi(g_{\frac{7}{2}}^8, d_{\frac{5}{2}}^4, d_{\frac{3}{2}}^1)\nu(f_{\frac{7}{2}})^1]$ 34.3%
6^-	290.6	284	-	-	$[\pi(g_{\frac{7}{2}}^8, d_{\frac{5}{2}}^5)\nu(f_{\frac{7}{2}})^1]$ 98.4%
1^-	383.3	385	-	-	$[\pi(g_{\frac{7}{2}}^7, d_{\frac{5}{2}}^6)\nu(f_{\frac{7}{2}})^1]$ 82% + $[\pi(g_{\frac{7}{2}}^7, d_{\frac{5}{2}}^4, d_{\frac{3}{2}}^2)\nu(f_{\frac{7}{2}})^1]$ 13.3% + $[\pi(g_{\frac{7}{2}}^7, d_{\frac{5}{2}}^4, d_{\frac{3}{2}}^1)\nu(f_{\frac{7}{2}})^1]$ 10.7%
$(3)^-$	420.88				
$(2)^-$	496.42				
$(2)^-$	689.3				
$(2)^-$	917.9				

levels of this nucleus, produced from the EC decay of ^{146}Gd , have been significantly modified from the singles decay and γ - γ coincidence measurements. The lifetimes of the two excited states have been measured following the Mirror Symmetric Centroid Difference technique using $\text{LaBr}_3(\text{Ce})$ detectors. The first 3^- and 2^- levels have been assigned to the lifetime values of 5.38 ± 1.8 and 8.38 ± 1.6 ps respectively. A Shell model calculation has been performed using OXBASH code considering ^{132}Sn as a core nucleus. The theoretical calculation agrees well with the experimental data. The level spectra and the lifetime values of the first two excited states along with the shell mode calculation establish the near spherical structure of ^{146}Eu vis a vis the validity of $Z = 64$ subshell closure for $N = 82$ closed shell nuclei. The measurements of quadrupole moments for the excited states of the nuclei in this mass region are under active consideration and this will give

more direct evidence regarding the systematics of the structure for the nuclei around the discussed shell closure.

VI. ACKNOWLEDGEMENT

The authors acknowledge the efforts of the operators of K=130 Cyclotron of Variable Energy Cyclotron Centre for providing a good quality beam. One of the authors (T. Malik) is thankful to Head, Physics Group, VECC and Head of the Department, Department of Applied Physics, Indian School of Mines, for allowing him to carry his winter project in VECC during the period December 2012 to January 2013. The authors acknowledge the sincere efforts of P. Mukhopadhyay, R. K. Chatterjee and A. Ganguly who have assisted meaningfully in this work and all the members of physics laboratory, VECC for the maintenance of the detectors throughout the year.

-
- [1] P. Jentschel *et al.*, Phys. Rev. Lett. **104**, 222502 (2010).
[2] P. E. Garret *et al.*, Phys. Rev. Lett. **103**, 062501 (2009).

- [3] A. Chakraborty *et al.*, Phys. Rev. Lett. **110**, 022504 (2013).

- [4] Tumpa Bhattacharjee *et al.*, Nucl. Phys **A750**, 199 (2005).
- [5] T. Bhattacharjee *et al.*, Nucl. Phys. A825, 16 (2009).
- [6] Tumpa Bhattacharjee *et al.*, Phys. Rev. **C78**, 024304 (2008).
- [7] Somen Chanda *et al.*, Phys. Rev. **C79**, 054332 (2009).
- [8] H. Mach, R.L. Gill and M. Moszynski, Nucl. Instr. & Meth. in Phys Res **A280**, 49 (1989).
- [9] H. Mach *et al.*, Nucl. Phys. **A523**, 197 (1991).
- [10] J.-M. Regis *et al.*, Nuclear Instr. & Meth. Phys. Res., **A622** 83 (2010).
- [11] P. Kleinheinz *et al.*, Z. Phys. **A290**, 279 (1979).
- [12] L. K. Peker and J. K. Tuli, Nucl. Data Sheets **82**, 187 (1997).
- [13] L. Holmberg *et al.*, Z. Physik **257**, 101 (1972).
- [14] R. Kantus, U. J. Schrewe, and W. -D. Schmidt-Ott Phys. Rev. **C23**, 1274 (1981).
- [15] A. Ercan *et al.*, Z. Physik **A295**, 197 (1980).
- [16] A. Ercan *et al.*, Z. Phys. **A329**, 63 (1988).
- [17] E. Ideguchi *et al.*, Eur. Phys. J. **A6**, 387 (1999).
- [18] H. Langevin-Joliot *et al.*, Phys. Rev. **C38**, 1168 (1988).
- [19] <http://www.nndc.bnl.gov/logft/>
- [20] B. A. Brown *et al.*, the computer code OXBASH, MSU-NSCL Report No. **524** (1994).
- [21] [www.tifr.res.in/ lamps](http://www.tifr.res.in/lamps).
- [22] Agda Artna-Cohen, Nucl. Data Sheets **79**, 1 (1996).
- [23] B. A. Brown and B. H. Wilden thal, Ann. Rev. Nucl. Part. Sci. **38** 29 (1988).
- [24] Hosaka *et al.*, Nucl Phys. **A444**, 76 (1985).